



Review of Bidirectional DC-DC Converters and Trends in Control Techniques for Applications in Electric Vehicles

Erik Martinez-Vera , *Student Member, IEEE*, and Pedro Bañuelos-Sanchez , *Member, IEEE*

Abstract—This paper comprehensively reviews bidirectional DC-DC converters and their control techniques for Electric Vehicle applications. A classification is proposed based on the three power ratings levels of the SAEJ1772 standard. Circuit topologies are compared based on power rating, switching frequency, static voltage gain, operating modes, number of components and power switch material. High switching-frequency topologies that include emerging Wide Bandgap (WBG) devices are also discussed. Cost comparison of traditional Si power switches and WBG devices employed in the reviewed topologies is also included. Traditional control methods for power converters in EVs are presented while also considering the emergence of Artificial Intelligence algorithms applied in systems controls that offer alternative methods to improve the efficiency of bidirectional DC-DC converters.

Link to graphical and video abstracts, and to code: <https://latam.ieceer9.org/index.php/transactions/article/view/8288>

Index Terms—Bidirectional Power Flow, DC-DC Power Converters, Control Systems, Electric Vehicle, Wide Bandgap Power Device, Artificial Intelligence

I. INTRODUCTION

The current transportation model is not sustainable due to its significant dependence on fossil fuels. To alleviate this problem, Electric Vehicles have been developed. On a global scale, 193 countries and the European Union (EU) joined the Paris Agreement, which aims to avoid a global temperature increase of more than 1.5 degrees Celsius above pre-industrial levels [1]–[4]. One of the leading greenhouse gases (GHG) is Carbon Dioxide (CO₂) which represents as much as 80% of the GHG emission, and 35% of that is related to transport activities [5], [6]. The U.S. plans to reduce its carbon footprint in transportation and attain fully decarbonized electricity by 2035 [7]. Germany plans to be GHG neutral by 2050 [8], [9]. Toxic pollutants such as Nitrogen Oxides (NO_x) and particulate matter (PM) are also released into the atmosphere from the combustion of fossil fuels [10]–[12]. The adverse effects on health include cardiovascular and respiratory diseases [13]. Concentrations of these pollutants are higher in cities with more significant motor traffic [14]. Considering this, the UK government and the European Union have announced the end of sales of new cars powered by fossil fuels by 2030 [15] and 2035 [16], respectively. Even though the fleet of electric

Dr. Pedro Bañuelos-Sanchez and Erik Martinez-Vera are with Universidad de las Américas-Puebla, México (e-mail: pedro.banuelos@udlap.mx and erik.martinezva@udlap.mx).

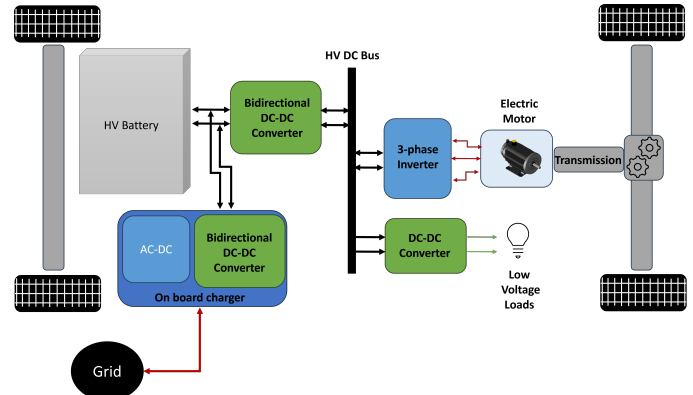


Fig. 1. Simplified block diagram of the powertrain in an EV.

cars represented only 1% of the total market [17], recent global sales of new EVs have more than doubled [18]. Hybrid Electric Vehicles (HEV), Plug-in Hybrid Electric Vehicles (PHEV) and Battery Electric Vehicles, or EVs, are subject to substantial investments for further improvement. One thing they have in common is using power electronics to manage power flow from the energy sources to the motors, ancillaries and electronic control units (ECU). Power Electronics devices are considered critical enablers of current advances in vehicle electrification [19]. Their importance derives from linking several components with different voltage ratings to a single energy source. Current can be bidirectional, flowing from the source to the load or vice versa. For example, an electric motor becomes a generator charging the battery during braking. The principal components of power electronic devices are the semiconductor switches, i.e. diodes or transistors, and proper component selection will significantly improve the converter performance [20]. Fig. 1 shows a simplified block diagram of the powertrain of an Electric Vehicle. The typical power system for an EV consists of a high-voltage battery, high-voltage wire harnesses or bus bars, an inverter, a charger and DC/DC converters. The high-voltage (HV) bus typically ranges from 250 VDC up to 450 VDC connecting the battery, chargers and electric motors [21], [22]. Still, 800 VDC systems have been developed to reduce ‘range anxiety’ and charging times [23], [24].

Bidirectional converters can be derived from the basic buck and boost DC-DC converters where the load voltage varies with the duty cycle of the main power switch [20], [25], [26]. Passive elements in the converter, such as capacitors

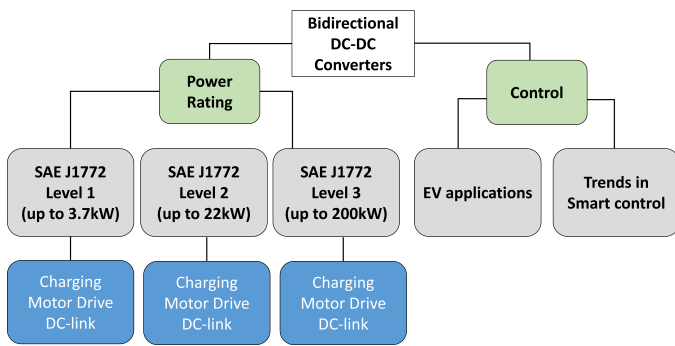


Fig. 2. Flow chart of the DC-DC Bidirectional converters review.

and inductors, increase in size and cost as the switching frequencies decrease; then, high switching frequencies are desired to obtain higher power densities and lower prices. However, increasing the frequency also increases the switching losses with reduced efficiency. Soft switching techniques have been developed to solve this, such as zero voltage switching (ZVS) or zero current switching (ZCS), but at the cost of increased circuit complexity. Also, WBG semiconductor materials such as Silicon Carbide (SiC) and Gallium Nitride (GaN) present an alternative to the traditional power switches made with Silicon (Si). Higher power output and higher operating frequencies of SiC and GaN allow to decrease switching losses and reduce the size of passive components compared to conventional IGBT and MOSFET devices. Si power electronics is a mature technology allowing it to fully integrate the power and control circuitry in a single chip, while WBG materials integration and packaging are still not fully developed, resulting in more expensive devices [27], [28]. Different reviews cover a substantial number of converters classifying them by type of power switch, power rating, topology, frequency of operation and various applications [27]–[33]. This paper reviews bidirectional DC-DC converters and their control techniques with a specific focus on applications in power systems of EVs. It is organized as follows: section II presents a review of bidirectional converters classified by power rating, section III reviews control techniques applied for bidirectional converters in EVs as well as emerging Artificial Intelligence (AI) control methodologies for power converters, section IV analyses both previous sections and section V provides conclusions of the trends identified within the document. Fig. 2 presents the flow diagram of this work.

II. POWER RATING CLASSIFICATION OF BIDIRECTIONAL DC-DC CONVERTERS

A standard classification for bidirectional converters is based on the presence of isolation, either through a transformer or a coupled inductor, regardless of the application [26], [29], [32], [33]. Fig. 3 and Fig. 4 show general setups of bidirectional DC-DC converters in EVs. Isolated topologies are required for the onboard charger to provide galvanic isolation and Vehicle to Grid (V2G) capabilities. However, bidirectional topologies without isolation are also designed for EVs where the converter is interfacing between the battery and the motor, also shown in the figures [34]. Hybrid configurations

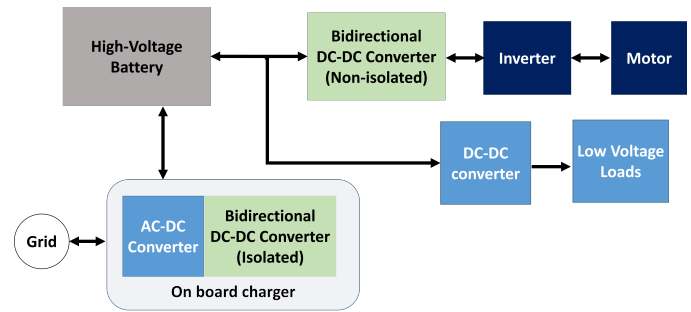


Fig. 3. General Setup of Bidirectional DC-DC converters in power systems of EVs - single power source system.

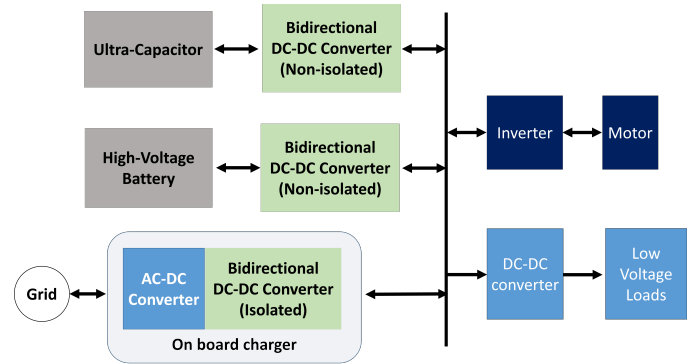


Fig. 4. General setup of Bidirectional DC-DC converters in power systems of EVs - hybrid energy storage system.

include an additional converter allowing Ultra-Capacitors (UC) to provide extra power during peak power demand, store braking energy, or receive power from the battery [35]. Multi-input/output topologies propose a single converter to interface between multiple energy sources and loads to avoid using multiple converters [36]–[39]. From both figures, bidirectional converters can be used with or without isolation in EVs; then, to provide a different point of view, classification is applied according to the power levels of the SAEJ1772 standard. This classification will allow obtaining a different perspective from the traditional classifications based on isolation, topology, or those focusing solely on charging applications. According to this standard, onboard chargers for EVs can be classified as Level 1 (up to 3.7 kW), Level 2 (3.7 - 22 kW) and Level 3, which is divided into Level 3 AC (22 to 43.5 kW) and Level 3 DC (up to 200 kW, fast charging) [31]. Different standards specify the power ratings for connectors as the SAE J1772-US [40], the IEC 62196-Europe [41] or the GB/T 20234-China [42]. CHAdeMO 2.0 charging protocol specifies high power charging up to 400 kW, while the recently released CHAdeMO 3.0/ChaoJi charging protocol allows up to 900 kW at 600 A and 1.5 kV [43]. The following subsections present a classification of bidirectional converters based on the three power rating levels of the SAEJ1772 standard with comparisons based on topology, power rating and switching frequency, among other metrics.

A. Level 1 (up to 3.7 kW)

The main applications of bidirectional DC-DC converters in EVs are charging, DC connection, propulsion and Cell-balancing. According to the intended application, diverse converter topologies have been developed to reduce switching losses while increasing power rating, frequency, power density and efficiency. Table I summarises the characteristics of bidirectional converters at Level 1, such as power rating, switching frequency, topology, static voltage gain, number of components and intended application. Topologies with output voltages of 400 VDC address current popular EV models [21], [22]. 800 VDC output voltage topologies are also under development to increase the EV range [44], [45]. A wide voltage range with low parts count is preferred to increase power density and reduce cost. However, interleaved and multilevel topologies with more switches provide less voltage stress on the components [45]–[47]. There is a clear tendency to develop topologies with WBG switches. GaN devices allowed for increasing the switching frequency up to 1 MHz [48], [49]. For charging applications, galvanic isolation can be obtained through a transformer or a coupled inductor to provide a safety barrier between the outside energy source and the EV electric system. References [44], [49]–[53] are examples of topologies with isolation for EV charging. Still, topologies without isolation have also been proposed for charging [36], [47], [54]–[56]. One of the most popular isolated topologies for charging applications is Dual-Active-Bridge (DAB). It can work bi-directionally in step-up and step-down modes with high power density and efficiency [26]. He and Khaligh compared DAB to CLLC topologies showing that the half-bridge CLLC is more efficient and less costly than its DAB counterparts [51]. However, CLLC requires variable switching frequency to control energy transfer, thus making its design more complex. Fig. 5 shows full bridge DAB and CLLC topologies: resonant LC tanks are added to the DAB to obtain the CLLC topology. From Table I, the Static Voltage Gain (SVG) of several converters can be compared. The SVG of non-isolated topologies is a function of the duty cycle of the power switches. However, for non-isolated topologies, the SVG become more complex functions based on the phase shift between the input and output signals. The SVG column on the table allows us to evaluate the possible range of output voltage vs the number of components for each topology. For example, the converter in [47] has an extensive output voltage range with four modes of operation and eight power switches. In contrast, the topology in [45] has a similar output voltage range with only six power switches. However, it only provides two modes of operation. It is also important to mention that the number of diodes in the topologies is mostly zero without considering antiparallel ones. This reduction is because transistors have replaced them. Additional information can be obtained from the part number column in the table. It is provided for the semiconductor switches when experimental validation is achieved. From them, cost evaluation and analysis can be provided in the section “IV Analysis and Discussion of Bidirectional Converters” of this paper.

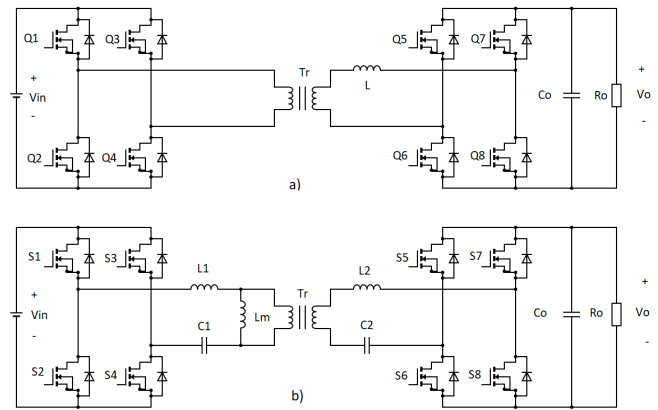


Fig. 5. Bidirectional Isolated topologies, a) Dual Active Bridge (DAB), b) CLLC [51].

B. Level 2 (3.7 kW up to 22 kW)

The previous section’s input/output voltage levels are also used for the SAE Level 2 power ratings; higher currents are needed to increase the power rating. These result in higher current ripples in the passive components and higher stress in the power switches. Higher rating components will be needed, which adds to the overall cost of the converter. A popular method to solve this issue is to apply interleaving to the bidirectional buck-boost topologies described before. Fig. 6 and Fig. 7 show two topologies with interleaving for ripple reduction. Fig. 6 displays two interleaved half-bridges with device paralleling, Quasi-Square-Wave (QSW) and ZVS [59]. Fig. 7 shows an isolated three-phase CLLC in combination with a four-level interleaved buck [60]. Similarly, a Quasi-resonant (QS) isolated four-level interleaved flyback is proposed in [61]. Different alternatives have also been proposed to deal with the stress in the components at higher power. An Input Parallel – Output Series topology was designed from a buck-boost converter to reduce the voltage stress by connecting the load in series with the output, thus processing only a fraction of the total power [62]. A Saturation-Prevention-Algorithm (SPA) was proposed for a DAB topology to increase power density [63]. A smaller transformer can be used by maintaining it in the linear operating region avoiding saturation and current spikes. A three-level boost converter is used for a wide output voltage range at the DC-DC stage of a current rectifier [64].

Table II presents a summary of the characteristics of the converters at this power level. A clear trend to use SiC devices is observed at switching frequencies higher than 100kHz. Also, interleaved are the most common topologies. It is essential to mention that these converters can be used as building blocks for higher power converters that comply with fast charging standards such as CHAdeMO. Table I and Table II show an increase in the average number of components. The average number of power switches in the previous section was five. In this section, the average increased to eight. This increase is likely related to the adoption of interleaving and multilevel. Also, most of the topologies are designed for higher input/output voltages which relate more to EV

TABLE I

SUMMARY OF SAE LEVEL 1 BIDIRECTIONAL POWER CONVERTERS (*L – INDUCTORS, C – CAPACITORS, D – DIODES, S – TRANSISTORS), (– NOT SPECIFIED)

Application	Power [W]	Switching frequency [kHz]	Operation mode	Topology	Static Voltage Gain	V_{in}	V_{out}	Number of Components			Power Switch	Part Number	
								L	C	D			S
Charging [50]	320	40	buck forward boost reverse	Coupled inductor	$\frac{2+n-d}{1-d}$	380	48	2	2	0	3	SiC	SCT3022AL
Charging DC-link [47]	1100	25	buck forward boost forward buck reverse boost reverse	two-phase interleaved cascade voltage doubler	$\frac{2}{1-d}$ d	150	25-1050	2	2	0	8	SiC Si	IRF4868 C2M0025120D
Charging DC-link [49]	1200	1000	buck forward boost reverse	interleaved inverse coupled inductor	$\frac{d}{1-d}$	380	150	2	4	0	4	GaN	–
Charging [44]	3300	100	buck forward boost forward buck reverse boost reverse	isolated half-bridge three-level rectifier series-resonant	$\frac{2[1+\frac{2(\sin\theta)^2}{Q\pi}]}{1+\cos\theta}$	370	640-840	3	4	2	8	SiC	SCH2080KE
Active cell balancing [57]	60	250	buck forward boost reverse	active clamp forward converter	$\frac{n_2 v_1}{n_1 L \Gamma_1 s + n_2 v_1}$	12	3.6	2	1	0	4	–	–
Charging [51]	1000	170	buck forward boost forward buck reverse boost reverse	Full-Bridge CLLC Half-Bridge CLLC Full-Bridge DAB Half-Bridge DAB	$\frac{1R_0d(1-d)}{n_2 f_s L}$	500	200 - 4 00	3 3	3 5	0 4	8 4	SiC	C2M0080120D
Propulsion [58]	250	100	buck forward boost reverse	bidirectional half-bridge	$\frac{d}{1-d}$	48	6	1	2	0	2	–	–
Charging [54]	200	30	buck forward boost reverse	double inductor double boost synchronous rectifier	$\frac{d^2}{(1-d)^2}$	180	12	2	2	0	4	Si	IRFP460 IRFP260
Propulsion DC-link [46]	1000	100	boost forward buck reverse	switched-inductor switched-capacitor synchronous rectifiers	$\frac{d}{4}$ $\frac{4}{1-d}$	24	400	2	5	0	6	–	–
Propulsion DC-link [45]	2000	100	buck forward boost reverse	interleaved voltage quadrupler	$\frac{d}{4}$ $\frac{4}{1-d}$	50-100	800	2	5	0	6	GaN	GS66516B -E01-MR
Charging [56]	500	50	boost forward buck reverse	two inductors common ground	$\frac{d^2}{2-d}$ $\frac{1+d}{(2-d)^2}$	40	200	2	4	0	5	Si	IPW60R099CPA

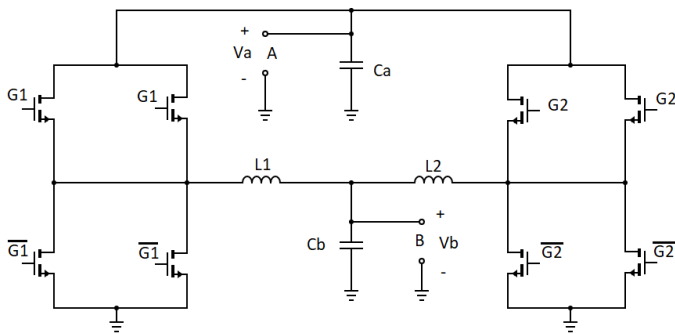


Fig. 6. Bidirectional Topology with two interleaved half bridges and device paralleling [59].

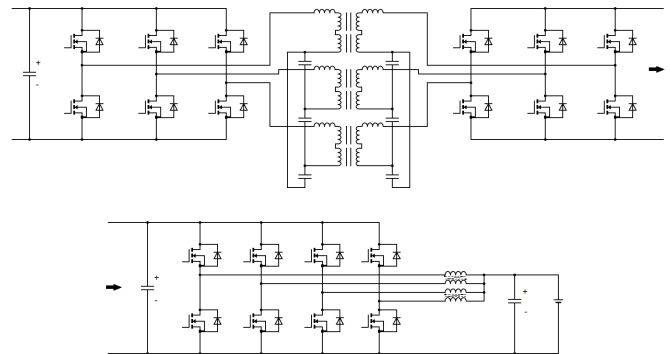


Fig. 7. Bidirectional Topology with top) 3-phase CLLC rectifier and bottom) 4-phase interleaved buck [60].

propulsion and charging applications. It must also be noted that, in the previous section, the highest switching frequency corresponded to a topology with GaN devices at 1 MHz [49]. In this section, the highest switching frequency is only 500 kHz with SiC devices [60]. However, there is a difference in operating power of almost an order of magnitude: from 1.2 kW to 12.5 kW.

C. Level 3 AC (22 to 43.5 kW) and DC (up to 200 kW)

Higher power ratings can be achieved with low-part-count topologies by adequately selecting the power switches and passive components. Up to 80 kW operating power was reported in [66] (Table III), with the cascade topology presented in the previous section (Table II) [65]. However, more expensive components will be required to cope with the more significant current and voltage ripples. Interleaving was mentioned earlier

TABLE II

SUMMARY OF SAE LEVEL 2 BIDIRECTIONAL POWER CONVERTERS (*L – INDUCTORS, C – CAPACITORS, D – DIODES, S – TRANSISTORS), (– NOT SPECIFIED)

Application	Power [kW]	Switching frequency [kHz]	Operation mode	Topology	Static Voltage Gain	V_{in}	V_{out}	Number of Components				Power Switch	Part Number
								L	C	D	S		
Charging DC-link [62]	3.75	20	boost forward buck reverse	Partial-power (Parallel - Series)		200	1500	4	4	0	8	Si	–
Charging propulsion/ DC-link [59]	5.4	450	buck forward boost reverse	interleaved device paralleling	$d, \frac{1}{1-d}$	400	270	2	2	0	8	GaN	GS66508T
Charging [60]	12.5	500	buck forward boost reverse	3-phase CLLC 4-p interleaved	Phase shift variable freq	850	200-800	7	9	0	20	SiC	IMZ120R045M1 C3M0075120K
Charging [63]	6.6	125	buck forward boost forward buck reverse boost reverse	DAB	Phase Shift	380-480	320-450	3	2	0	8	SiC	C3M0065090J
Propulsion [65]	20	15	buck forward boost forward buck reverse boost reverse	two topologies: -buck-boost -cascade buck-boost	$d, \frac{1}{1-d}$	180	720	1	2	0	2,4	Si	–
Charging [64]	10	100	buck forward boost forward buck reverse boost reverse	3-level boost	–	325	200-1000	2	2	0	4	SiC	C3M0010090K
Charging [61]	10	350	buck forward boost forward buck reverse boost reverse	interleaved flyback	$-\frac{2}{d}(f_{sw}T_F - 1 + d)$	50-500	750	3	12	6	8	SiC	C2M0080120D

as a solution to overcome large current ripples and was implemented in [67] and [68] for a 30 kW converter. Using SiC increased the switching frequency from 20kHz to 60 kHz with a reduction of 63% in semiconductor power losses compared to Si devices [67]. Thus, the size of passive components and cooling equipment could also be reduced. The trend to employ SiC devices with interleaved topologies and a wide voltage range can be observed. A 200 kW power converter for a wide voltage range is presented in [69] for charging applications; however, more information needs to be provided about the topology or type of semiconductor material. Table III summarises the features of SAE Level 3 DC converters. Two converters were included with power ratings of 360 kW [70] and 400 kW [71] as examples of devices compliant with CHAdeMO charging levels.

III. CONTROL OF BIDIRECTIONAL CONVERTERS

Control techniques for voltage converters are a research topic, with entire books or sections of books dedicated to the subject. Detailed descriptions and derivations of a variety of control methodologies are already accessible in the literature [20], [72], [73]. The main complexity in bidirectional DC-DC converter control derives from having to regulate, in two directions, the flow of power [26]. PID is the elementary control method. However, since the converter has nonlinear behaviour, complex stability analysis or linearization around an operating point must be implemented to improve its performance. Different approaches have been proposed to overcome these problems. Pulse Width Modulation (PWM) is a commonly used technique that can be divided into voltage-mode control (VMC) and current-mode control (CMC) [30]. Both methods have been compared for a buck converter [74].

Soft-switching (SS) techniques are used to minimize switching losses in semiconductor devices [44], [60]. Phase-shift control (PS), two-edge-modulation (TEM) and space-vector-modulation (SVM) have also been proposed for converter control [75]. Sliding mode control (SMC) is a nonlinear capable method that is less affected by changes in the load [76], [77]. Model Predictive Control uses a model of the converter to predict the future output and future error; then, an online optimization function is used to estimate the following input into the controller [78], [79]. Fuzzy Logic (FL) is considered a robust controller for a DC-DC converter: easy to implement with little knowledge of the system. It works with nonlinear systems and has minor sensitivity to load disturbances [80]. Different Control methods can be implemented in Digital Signal Processors (DSP) or Field Programmable Gate Arrays (FPGA), providing flexibility for the designer [79], [81]. Artificial Intelligence (AI) is emerging as a potential application in the field of power systems [82]–[84]. Then, in the following subsections, a review is performed of applications of control techniques with a focus on EV applications and methodologies that use AI-based control algorithms.

A. EV Applications

Due to its simplicity and robustness, the most popular method for converter control in EV applications is the Proportional Integral Derivative (PID). Voltage Mode Control (VMC) PID is the standard control for buck converters, yet, boost converters are highly nonlinear. Then, an inner control loop needs to be added to the basic PID configuration. Peak Current Mode Control (PCMC) is usually added as an inner PID loop to cope with the nonlinearity of the converter [85]. Several examples can be found of PID for EV applications. Two independent PID branches control the buck and boost modes

TABLE III

SUMMARY OF SAE LEVEL 3 BIDIRECTIONAL POWER CONVERTERS (*L – INDUCTORS, C – CAPACITORS, D – DIODES, S – TRANSISTORS), (– NOT SPECIFIED)

Application	Power [kW]	Switching frequency [kHz]	Operation mode	Topology	Static Voltage Gain	V_{in}	V_{out}	Number of Components				Power Switch	Part Number
								L	C	D	S		
Charging propulsion DC-link [66]	80	20	buck forward boost forward buck reverse boost reverse	half-bridges vs. middle inductor	$d, \frac{1}{1-d}$	300	650	1,2	2,3	0	4	Si	–
Propulsion DC-Link [67]	30	60	boost forward buck reverse	2-level 3-phase interleaved	–	324	400-700	3	2	0	6	SiC	CAS120M12Bm2
Propulsion DC-Link [68]	30	60	boost forward buck reverse	2-level 3-phase interleaved	–	250-370	400	3	2	0	6	SiC	CAS120M12Bm2
Propulsion DC-Link [70]	360	100	–	6-phase half-bridge	–	20-850	10-850	6	2,3	0	12	SiC	–
Charging [69]	200	–	buck-boost	–	–	10-1150	60-1200	–	–	0	–	–	–
Propulsion [71]	400	–	–	4-q rectifier	–	–	20-800	–	–	–	–	–	–

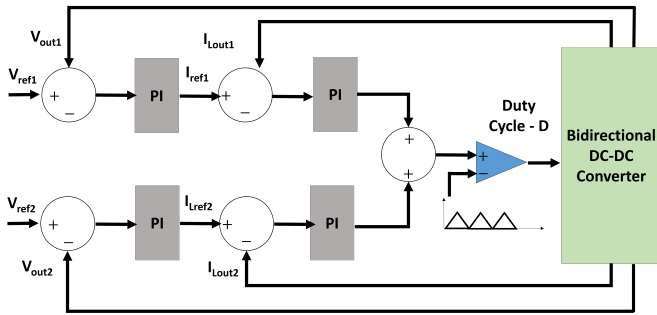


Fig. 8. PWM generator with four PI control blocks for a dual-input dual-output converter [38].

of operation when charging/discharging an ultra-capacitor in a hybrid energy storage system [35]. Four proportional-integral (PI) loops in parallel control the current and voltage of a converter during battery charging/discharging [61]. A multi-input converter uses two inner loops to control the voltage and current of the converter, while a third outer loop controls the output power [37]. A dual-input dual-output converter employed cascaded PI stages to regulate the input from a PV panel and a battery. The block diagram is shown in Fig. 8 [38]. An isolated onboard charger with a high-frequency transformer and interleaved DC stage implemented three parallel PI branches [52]. Three PI control loops generated four PWM duty cycles in a four-switch single-input three-output bidirectional buck converter [39]. Unpredictable operation in the buck and boost modes of the converter in an EV poses a problem for linear controllers; then, nonlinear Time Domain Control (TDC) is proposed and compared against PI, observing reduced voltage overshoots and faster settling times [85]. PI can also be applied with other methods: a digital dead-beat controller is implemented with a PI compensator to select from constant-current or constant-voltage charging modes [56].

Other control methods have also been applied to power converters. Pulse Frequency Modulation was implemented for an off-board charger designed for EVs connected to microgrids [53]. MPC is applied to regulate the individual voltages of cells inside the battery pack of an EV [78]. A fuzzy logic

control, an interval type-2 fuzzy logic control and a real-coded genetic algorithm rule-based fuzzy logic controller were implemented for the shunt converter of a bidirectional EV charging system [80]. A comparison between SMC and FL is presented in [86] for a DAB converter. A linearized model of the system is derived for SMC output current control, while a model-less approach is implemented for the FL control. Fuzzy Logic was also implemented for a bidirectional converter in hybrid energy storage with a battery and a supercapacitor [87]. Simulation results are compared against benchmark PI showing better transient response for the FL approach. Table IV summarizes the control methods for power converters in EV applications and general-purpose applications. The latter are reviewed in the following subsection. Like the previous sections, most converters are rated Level 1, low power and low voltage. The average number of power switches is seven, with a maximum of sixteen. The most frequent control method is PI, the benchmark for comparison against more complex methods. FL is the second most frequent control method for EV applications. The highest switching frequency is 350 kHz with SiC devices; the average is 75 kHz, mostly with Si devices. Again, the same trend can be observed as in the previous section, where most of the designed converters are low power, low voltage and low frequency. Even though they present innovative topologies, they must be validated at commercial power levels before market adoption.

B. Trends in Smart Control

Most of the bidirectional converters in the previous section apply some PI control methodologies. Examples that compare Fuzzy Logic against PI and SMC show better transient responses. Therefore, it is essential to review emerging alternative AI methodologies already applied to general-purpose DC-DC power converters. The lower section of Table 4 summarizes the features of AI control methods for general-purpose power converters. Kurokawa et al. propose model control and neural network digital control methods for a multiple-output DC-DC converter with PID as a feedback control [89]. This network predicts the output voltage using six hidden layers and a sigmoid function at the output layer as the topology

TABLE IV
SUMMARY CONTROL METHODS FOR POWER CONVERTERS (*L – INDUCTORS, C – CAPACITORS, D – DIODES, S – TRANSISTORS), (– NOT SPECIFIED)

Application	SAE Power Level	Switching frequency [kHz]	Bidirectional	Topology	Control Mode*	V_{in}	V_{out}	Number of Components				Power Switch	Part Number	Settling Time [s]
								L	C	D	S			
Charging DC-link [36]	1	20	Yes	three-level three-port	PI	36	25	2	2	2	4	–	–	–
Propulsion DC-link [35]	1	10	Yes	Series Hybrid energy Storage	PI	16	28	1	1	1	2	Si	IRL2505	–
Propulsion DC-link [37]	1	20	Yes	single inductor switched-capacitors	PI	12	72	1	6	0	10	–	–	–
Propulsion DC-link [38]	1	10	Yes	Double input/output	PI	12	58	2	3	2	3	Si	IRFP250N	–
Charging [52]	1	10	Yes	interleaved 2 full wave rectifiers	PI	300	120	2	3	12	12	–	–	$\approx ms$
DC-link [39]	1	50	Yes	three output	PI	48	12, 5	3	3	0	4	–	–	–
Charging [53]	1	70	Yes	3 level CLLC resonant converter	PI	750	200-700	2	10	8	16	Si	IPZA60R037P7	$\approx \mu s$
Charging [56]	1	50	Yes	2 inductors common ground	PI	40	200	2	4	0	5	Si	IPW60R099CPA	$\approx ms$
Charging [61]	2	350	Yes	interleaved flyback	PI	50-500	700	3	12	6	8	SiC	C2M0080120D	–
Cell Balance [78]	1	250	Yes	Active clamp forward converter shunt converter	MPC	12	4/2	1	2	0	8	–	–	–
Charging [80]	2	10	Yes	DAB	T1, IT2, RCA FL	415 AC	700 DC	3	1	0	6	–	–	$\approx ms$
Charging [86]	2	100	Yes	DAB	FL vs SMC	270	28	2	2	0	8	Si SiC	SCH2080-KE IRFP4568 - PBF	$\approx ms$
Charging [87]	1	–	Yes	2-input hybrid energy storage	FL vs PI	100	40	2	1	2	4	–	–	–
Charging [85]	1	30	Yes	boost/buck	TDC vs PI	18	24	1	2	0	2	–	–	8ms 4%OV
General purpose [79]	1	1000	Yes	Buck/boost	MPC with NN	40/60	24/30	1	1	0	2	GaN	GS66506T	15μs 13.3%OV
General purpose [88]	1	1000	No	boost	SDC vs PI	1	1.67	1	1	0	2	–	–	6μs 4.7%OV
General purpose [89]	1	200	No	two-output buck	PID with NN	36	5	2	2	5	1	–	–	0.08ms 0.4%OV
General Purpose [90]	1	–	Yes	buck, boost, buck/boost	PID vs NN	30/12	5/25	1	1	1	1	–	–	5ms 25%OV
General purpose [91]	1	20	No	boost	DHP-NN vs PI	60	200	1	1	1	1	–	–	25ms 5%OV
General purpose [92]	1	1000	No	buck	MPC with NN	48	24	1	1	0	2	GaN	–	9μs 2.1%OV

PI –proportional integral, MPC – model predictive control, T1 – type 1, IT2 – interval type 2, RCA –real genetic algorithm, FL – fuzzy Logic, SMC – sliding mode control, TDC – time delay control, NN – neural networks, SDC – stochastic duty cycle, DHP – dual heuristic programming, OV/UV - overshoot/undershoot.

of the neural network. Backpropagation with 1000 readings generated with a conventional controller feeds the network for training to derive the ON time of the power switch. Comparison with a PID controller shows a faster transient response and lower voltage overshoot to step changes in the load. Neural Network (NN) control for buck, boost and buck-boost topologies using an online backpropagation algorithm was implemented in [90]. NN has a lower overshoot and fewer oscillations than PID, with good dynamic performance adapting to disturbances in the input voltage. A dual heuristic programming (DHP) method is proposed to control the voltage of a boost converter working in continuous and discontinuous current conduction mode (CCM and DCM, respectively) [91]. The DHP uses two NN: an action network to control the system and a critic network to assess the performance of the action network. Compared to PI, the DHP results in less overshoot and lower settling times without using an exact system model.

A buck topology with GaN devices at 1 MHz switching frequency and explicit MPC is implemented in [79]. A NN is used to map the nonlinear behaviour of the converter for varying operating points. Backpropagation is used to train the NN offline, which is then used to simulate and validate their

approach experimentally. Also, using GaN devices, FPGA and 1 MHz switching frequency, Chen et al. developed a real-time self-learning MPC control for a buck converter [92]. Their objective is to overcome the limits of high-frequency switching when updating the parameters of the MPC controller in real time. For this, a reward function is defined, and gradient descent updates the weights of a NN to optimize the duty cycle based on the previous performance of the converter.

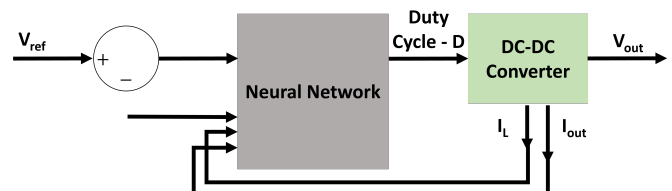


Fig. 9. Block diagram of NN Control for DC-DC converter (Based on [92]).

Fig. 9 shows the block diagram of the NN with a closed feedback loop; output voltage, Inductor Current and output current are feedback to the neural network along with the difference between the desired and actual output voltage. The NN weights are updated in real-time to estimate the optimal

duty cycle D . Finally, a stochastic method to derive the duty cycle (SDC) in Peak Current Mode Control (PCMC) for a boost converter is presented in [88] and compared against PI and robust PI. The right half-plane zero in the converter's small signal control-to-output transfer function results in an unstable system. To avoid complex solutions involving numerical methods, stochastic generation of the duty cycle allowed them to obtain more accurate and faster approximations of the optimal duty cycle than with traditional and robust PI. The lower section of Table IV summarises the AI control methods in power converters. It can be noted that all converters are general-purpose applications at low power and voltage. However, the average switching frequency is 644 kHz, and half the converters reach 1 MHz with GaN devices. Most converters have low parts count with a maximum of 2 power switches which means very basic unidirectional converters are used. NN are the most frequent control method. PID is also frequent but this time as the benchmark method for comparison. Then, AI methodologies mainly focused on the control design without considering the standard metrics of power converter performance, like power density or efficiency. Additionally, the last column of the table includes the settling time of the converters for comparison of the dynamic performance. It must be stated that the converters with EV applications report mostly their steady state performance. Its dynamic performance is mostly related to charging/discharging profiles. In comparison, the lower section of the table shows the control methods for general purpose applications where dynamic performance parameters are reported. As expected, the settling time is correlated to the switching frequency. Systems with higher switching frequencies are able to react more quickly to changes in the output which comes as an additional benefit from the adoption of WBG devices.

IV. ANALYSIS AND DISCUSSION OF BIDIRECTIONAL CONVERTERS

A summary of frequency vs power for the converters in the three levels of SAEJ1772 and up to 400kW for CHAdeMO is presented in Fig. 10. The semiconductor material of the power switches is also indicated, showing Si devices at the left side of the graph with wide-range power but low frequency: the average power for these converters is 11.2kW with 32.5kHz average switching frequency. SiC converters are located in the centre-right side of the graph with an average power of 42.2kW and an average frequency of 148.2kHz. Chakraborty *et al.* [67] state that a reduction of 63% in semiconductor power losses could be achieved by switching from Si to SiC while also being able to increase by a threefold the switching frequency. Then, the size of the passive components could be reduced, which in turn leads to an overall size reduction of the converter. It must be noted that the SiC converter in [70] is outside the SAEJ1772 standard but within the CHAdeMO 400kW level. Finally, GaN topologies present low power with an average of 2.1kW but very high frequencies with a mean of 562kHz up to a maximum of 1MHz.

Proper design and component selection can scale low-power topologies to higher power ratings. Still, large current ripples

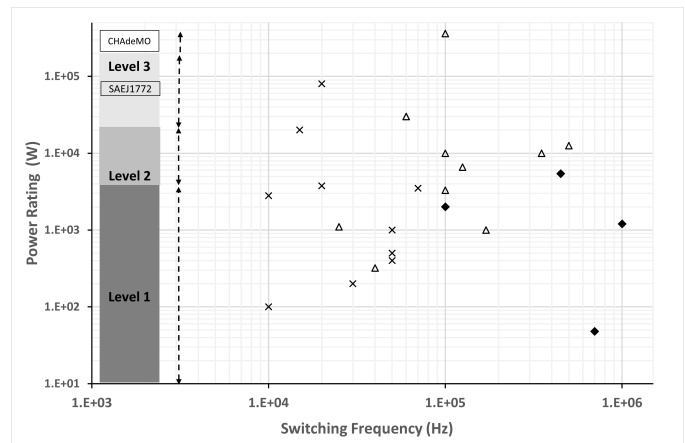


Fig. 10. Summary of Frequency vs Power of selected bidirectional converter topologies. χ – Si, Δ – SiC, *fulldiamond* – GaN.

will require more costly components. Interleaving is a popular method to split the current into several branches reducing the ripples and size of the components. The combination of interleaving with WBG devices increased the power rating to 200 kW with switching frequencies of 200 kHz [70]. GaN devices allow increasing the frequency even further with prototypes already a 1 MHz, although soft-switching techniques and snubbing circuits required to minimize switching losses complicate its design. Fu *et al.* [81] state that the increase in converter efficiency by switching from Si to GaN is minimal compared to the increase in cost; therefore, a significant increase in power density must be achieved to account for moving to WBG devices. Low power-level topologies present lower parts count since smaller current and voltage ripples are generated, which cheaper components can endure. However, higher current ripples will require more expensive components at higher power levels. Then, it might be preferable to increase the part count by including interleaving, or multilevel, which reduces stress in components. For widespread adoption of EVs, prices need to decrease significantly. For instance, in emerging economies, the starting price of the most popular EV brands can be four times those of the cheapest fossil-fuel-powered models [93]–[96]. Current prices render EVs as luxury items. Therefore, a combination of topology, components and control methods that achieves significant price reduction in power converters is necessary to reach the mass adoption of EV technology. Based on the power switch features indicated in tables I through IV, unitary prices for power switches were retrieved from [97]–[104] to perform a cost analysis. The results are shown in Fig. 11 for voltage rating vs unitary price and Fig. 12 for switching frequency vs unitary price. A clear gap can be appreciated between Si and SiC-GaN in terms of cost and voltage rating. While Si devices are the cheapest, they also have a limit of 600 V rating, while SiC devices reach up to 1.2 kV. Still, the price difference can be up to two orders of magnitude. Even though the voltage ratings are similar between GaN and Si, the price difference can be almost an order of magnitude for the WBG device. This difference can be explained by looking at the switching frequency in Fig. 12, where GaN has been applied up to 1 MHz while the

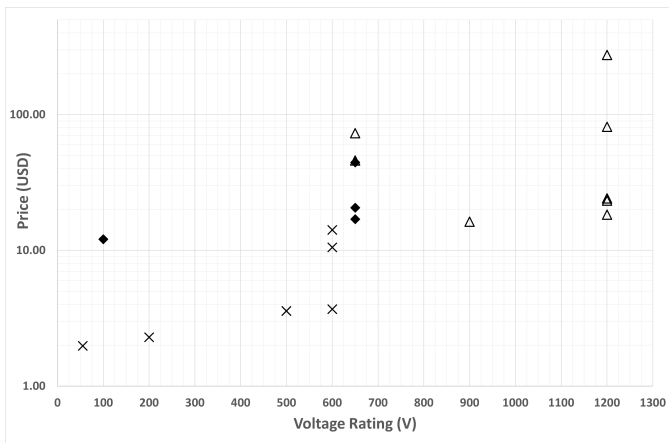


Fig. 11. Voltage-Rating vs Unitary price for $\chi - Si, \Delta - SiC, fulldiamond - GaN$ power switches [97]–[104].

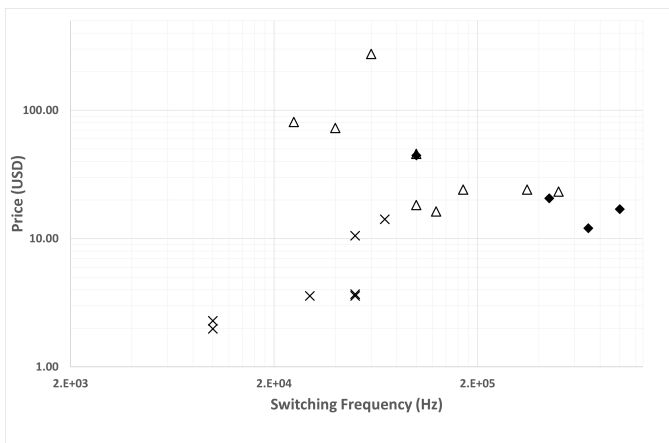


Fig. 12. Applied switching Frequency vs Unitary price [97]–[104] for $\chi - Si, \Delta - SiC, fulldiamond - GaN$ power switches.

most expensive Si is limited below 500 kHz.

Table IV summarizes the control methods of bidirectional power converters for EV applications and general-purpose converters. For EV applications, PI is the most popular control method and is the benchmark method for comparison with other approaches. However, MPC, FL and TDC have also been applied, showing better transients than PI. Most converters have SAEJ1772 level 1 power rating and use Si devices at switching frequencies below 90 kHz. The only two converters with a Level 2 power rating use SiC at frequencies above 90 kHz. Applications of Smart Control methods were found for general-purpose converters with or without bidirectionality. The most observed intelligent control method is NN control, alone or in combination with other approaches. Its performance is mainly compared against the benchmark PI showing lower voltage overshoots and faster settling times. Also, they can be implemented without strict, rigorous models, which eases the design procedure. However, most topologies are low power, low voltage and lack bi-directionality. GaN devices have been combined with intelligent control achieving switching frequencies up to 1 MHz, yet, at low power and with the most basic topologies. Then, an analysis of intelligent control methods combined with WBG devices at EV power

ratings needs to be carried out. The feasibility of significant cost reduction with higher power density must be evaluated.

V. CONCLUSIONS

A review of bidirectional DC-DC converters for applications in EVs has been presented in this work. Tables 1,2, and 3 summarize the power ratings, switching frequency, static voltage gain, and the number of components and materials of power switches for circuit topologies rated up to 200 kW and divided according to the three power rating levels of SAEJ1772. Converters up to 400 kW were also reviewed, which comply with CHAdeMO 2.0 protocol. Complex topologies are presented with low parts count to reduce costs and increase power density at low power levels. However, Wide output voltage range is also a desired feature which might be obtained at the cost of an increase in the number of components. Prototypes, including GaN devices, feature switching frequencies up to 1MHz, thus decreasing the size of passive components. However, interleaved topologies and SiC have become more popular at higher power levels to reduce volume despite the increase in parts count. Interleaved half-bridges are more popular for applications which work without isolation. Currently, PI is the most common control method due to its simplicity. However, several loops must be added to control the nonlinearities of the DC-DC converters. Fuzzy Logic and Neural-Networks have been applied with SiC and GaN devices at high-frequency low-power converters observing lower voltage overshoot and faster settling times than with PI. Moreover, higher switching frequencies allow an overall decrease in the settling time of the converter which, comes as an added benefit from WBG devices. A combination of intelligent control methods with WBG devices at EV power ratings needs to be evaluated to ascertain the cost-benefit relationship of these technologies.

ACKNOWLEDGEMENTS

This work was developed thanks to the funding from UDLAP Intelligent Systems Program and CONAHCyT PNCP.

REFERENCES

- [1] UNFCCC, “United nations framework convention on climate change,” 2021.
- [2] Secretaría de Gobernación, “Tratados Internacionales Celebrados por México - SRE,” 2021.
- [3] United Nations, “The Paris Agreement | United Nations,” 2022.
- [4] United Nations, “United Nations Treaty Collection - Paris Agreement,” 2015.
- [5] NASA-JPL, “Causes | Facts – Climate Change: Vital Signs of the Planet,” 2021.
- [6] US EPA, “Overview of Greenhouse Gases | US EPA,” 2017.
- [7] U. S. Office of the Press Secretary, “Fact Sheet: President Biden Sets 2030 Greenhouse Gas Pollution Reduction Target Aimed at Creating Good-Paying Union Jobs and Securing U.S. Leadership on Clean Energy Technologies,” 2021.
- [8] U. Kramer, “Defossilizing the Transportation Sector, Options and Requirements for Germany,” 2019.
- [9] UNFCCC | Germany, “Climate Action Plan 2050 | UNFCCC,” 2019.
- [10] EPA, “The Sources and Solutions: Fossil Fuels,” *Environmental Protection Agency*, pp. 1–5, 2021.
- [11] WHO, “About air quality and health,” 2021.
- [12] U.S. EPA., “Integrated science assessment (ISA) for oxides of nitrogen: Health criteria (Final report, Jan 2016),” tech. rep., U.S. Environmental Protection Agency, Washington, DC, mar 2016.

- [13] WHO, "Ambient (outdoor) air pollution," 2021.
- [14] Greenpeace, "Mapped: nitrogen dioxide pollution around the world - Unearthed," 2021.
- [15] UK DOT, "Government takes historic step towards net-zero with end of sale of new petrol and diesel cars by 2030 - GOV.UK," 2020.
- [16] ECEEE, "EU nations approve end to combustion engine sales by 2035," 2022.
- [17] Bloomberg, "EVO 2021," 2021.
- [18] L. Paolo and T. Gull, "Electric cars fend off supply challenges to more than double global sales - Analysis - IEA," 2022.
- [19] F. Blaabjerg, H. Wang, I. Vernica, B. Liu, and P. Davari, "Reliability of Power Electronic Systems for EV/HEV Applications," *Proceedings of the IEEE*, vol. 109, no. 6, pp. 1060–1076, 2021.
- [20] E. C. Dos Santos and E. R. Cabral da Silva, *Advanced Power Electronic Converters: PWM Converters Processing AC Voltages*. Hoboken, NJ, USA: John Wiley & Sons, Inc, nov 2014.
- [21] NISSAN, "2022 LEAF® OWNER'S MANUAL and MAINTENANCE INFORMATION," 2022.
- [22] Tesla, "Model S Owner's Manual," 2022.
- [23] L. Ulrich, "800-Volt EV Charging: The Other Palliative for Range Anxiety-IEEE Spectrum," 2022.
- [24] Porsche, "Porsche Taycan," 2022.
- [25] I. Batarseh and A. Harb, *Power Electronics: Circuit analysis and design*. SPRINGER INTERNATIONAL PU, 2017.
- [26] S. A. Gorji, H. G. Sahebi, M. Ektesabi, and A. B. Rad, "Topologies and Control Schemes of Bidirectional DC-DC Power Converters: An Overview," *IEEE Access*, vol. 7, pp. 117997–118019, 2019.
- [27] Y. Wang, O. Lucia, Z. Zhang, S. Gao, Y. Guan, and D. Xu, "A Review of High Frequency Power Converters and Related Technologies," 2020.
- [28] M. Parvez, A. T. Pereira, N. Ertugrul, N. H. E. Weste, D. Abbott, and S. F. Al-Sarawi, "Wide Bandgap DC-DC Converter Topologies for Power Applications," *Proceedings of the IEEE*, vol. 109, pp. 1253–1275, jul 2021.
- [29] A. Affam, Y. M. Buswig, A. K. B. H. Othman, N. B. Julai, and O. Qays, "A review of multiple input DC-DC converter topologies linked with hybrid electric vehicles and renewable energy systems," *Renewable and Sustainable Energy Reviews*, vol. 135, no. January 2020, p. 110186, 2021.
- [30] M. Z. Hossain, N. A. Rahim, and J. a/l Selvaraj, "Recent progress and development on power DC-DC converter topology, control, design and applications: A review," *Renewable and Sustainable Energy Reviews*, vol. 81, no. October 2017, pp. 205–230, 2018.
- [31] A. Khaligh and M. D'Antonio, "Global Trends in High-Power On-Board Chargers for Electric Vehicles," *IEEE Transactions on Vehicular Technology*, vol. 68, pp. 3306–3324, apr 2019.
- [32] F. Mumtaz, N. Zaihar Yahaya, S. Tanzim Meraj, B. Singh, R. Kannan, and O. Ibrahim, "Review on non-isolated DC-DC converters and their control techniques for renewable energy applications," *Ain Shams Engineering Journal*, vol. 12, pp. 3747–3763, dec 2021.
- [33] S. Alatai, M. Salem, D. Ishak, H. S. Das, M. A. Nazari, A. Bughneda, and M. Kamarol, "A review on state-of-the-art power converters: Bidirectional, resonant, multilevel converters and their derivatives," *Applied Sciences (Switzerland)*, vol. 11, no. 21, 2021.
- [34] A. Sheir, M. Z. Youssef, and M. Orabi, "A novel bidirectional T-type multilevel inverter for electric vehicle applications," *IEEE Transactions on Power Electronics*, vol. 34, no. 7, pp. 6648–6658, 2019.
- [35] P. Bhattacharyya, A. Banerjee, S. Sen, S. K. Giri, and S. Sadhukhan, "A Modified Semi-Active Topology for Battery-Ultracapacitor Hybrid Energy Storage System for EV Applications," *2020 IEEE International Conference on Power Electronics, Smart Grid and Renewable Energy, PESGRE 2020*, pp. 1–6, 2020.
- [36] A. Ganjavi, H. Ghoreishy, A. A. Ahmad, and Z. Zhagn, "A Three-Level Three-port Bidirectional DC-DC Converter," in *Proceedings - 2018 IEEE International Power Electronics and Application Conference and Exposition, PEAC 2018*, pp. 1–4, IEEE, nov 2018.
- [37] B. B. T. Shekin and K. Biju, "A Multi-Input Switched Capacitor Bidirectional DC-DC Converter with Triple Closed Loop Control for Electric Vehicle Application," *2021 IEEE International Power and Renewable Energy Conference, IPRECON 2021*, 2021.
- [38] K. Suresh, C. Bharatiraja, N. Chellammal, M. Tariq, R. K. Chakraborty, M. J. Ryan, and B. Alamri, "A Multifunctional Non-Isolated Dual Input-Dual Output Converter for Electric Vehicle Applications," *2021*, vol. 9, pp. 64445–64460, 2021.
- [39] M. Ramesh, B. Mallikarjuna, and T. Rajasekar, "A Novel Investigation on Single-Input Three-Output DC-DC Buck Converter For Electrical Vehicles," in *2021 7th International Conference on Electrical Energy Systems (ICEES)*, pp. 141–146, IEEE, feb 2021.
- [40] SAE International, "J1772 Electric Vehicle and Plug in Hybrid Electric Vehicle Conductive Charge Coupler," 2017.
- [41] IEC, "IEC 62823:2015 | IEC Webstore,"
- [42] China Government, "GB/T 20234.1-2015: PDF in English.," 2016.
- [43] CHAdeMO, "Protocol Development," 2022.
- [44] D. Yang, B. Duan, C. Zhang, Y. Shang, Y. Song, H. Bai, and Q. Su, "High-Efficiency Bidirectional Three-Level Series-Resonant Converter with Buck-Boost Capacity for High-Output Voltage Applications," *IEEE Transactions on Transportation Electrification*, vol. 7, no. 3, pp. 969–982, 2021.
- [45] H. Moradisizkoochi, N. Elsayad, and O. A. Mohammed, "A Voltage-Quadrupler Interleaved Bidirectional DC-DC Converter with Intrinsic Equal Current Sharing Characteristic for Electric Vehicles," *IEEE Transactions on Industrial Electronics*, vol. 68, no. 2, pp. 1803–1813, 2021.
- [46] R. Rezaei, M. Nilian, M. Safayatullah, S. Ghosh, and I. Batarseh, "A Bidirectional DC-DC Converter with High Conversion Ratios for the Electrical Vehicle Application," *IECON Proceedings (Industrial Electronics Conference)*, vol. 2021-October, 2021.
- [47] J.-H. Teng, S.-W. Chen, S.-W. Luan, and J.-R. Xu, "Bidirectional DC-DC Converter with a Wide-Range Voltage Conversion Ratio," in *2019 IEEE 4th International Future Energy Electronics Conference (IFEEC)*, pp. 1–6, IEEE, nov 2019.
- [48] N. T. Phan, A. D. Nguyen, Y. C. Liu, and H. J. Chiu, "An investigation of zero-voltage-switching condition in a high-voltage-gain bidirectional dc-dc converter," *Electronics (Switzerland)*, vol. 10, no. 16, 2021.
- [49] X. Huang, F. C. Lee, Q. Li, and W. Du, "High-Frequency High-Efficiency GaN-Based Interleaved CRM Bidirectional Buck/Boost Converter with Inverse Coupled Inductor," *IEEE Transactions on Power Electronics*, vol. 31, no. 6, pp. 4343–4352, 2016.
- [50] A. Ayachit, S. U. Hasan, Y. P. Siwakoti, M. Abdul-Hak, M. K. Kazimierzczuk, and F. Blaabjerg, "Coupled-Inductor Bidirectional DC-DC Converter for EV Charging Applications with Wide Voltage Conversion Ratio and Low Parts Count," in *2019 IEEE Energy Conversion Congress and Exposition (ECCE)*, pp. 1174–1179, IEEE, sep 2019.
- [51] P. He and A. Khaligh, "Comprehensive Analyses and Comparison of 1 kW Isolated DC-DC Converters for Bidirectional EV Charging Systems," *IEEE Transactions on Transportation Electrification*, vol. 3, no. 1, pp. 147–156, 2017.
- [52] O. Alkul and S. Demirbas, "A Novel High Frequency-Link Bidirectional DC-DC Converter for Electric Vehicle Applications," in *2019 2nd International Conference on Smart Grid and Renewable Energy (SGRE)*, pp. 1–6, IEEE, nov 2019.
- [53] Y. Xuan, X. Yang, W. Chen, T. Liu, and X. Hao, "A Novel Three-Level CLLC Resonant DC-DC Converter for Bidirectional EV Charger in DC Microgrids," *IEEE Transactions on Industrial Electronics*, vol. 68, no. 3, pp. 2334–2344, 2021.
- [54] S. S. S. Sethuraman, K. Santha, L. Mihet-Popa, and C. Bharatiraja, "A Modified Topology of a High Efficiency Bidirectional Type DC-DC Converter by Synchronous Rectification," *Electronics*, vol. 9, p. 1555, sep 2020.
- [55] A. Sharma, S. S. Nag, G. Bhuvaneshwari, and M. Veerachary, "Non-isolated bidirectional DC-DC converters with multi-converter functionality employing novel start-up and mode transition techniques," *IET Power Electronics*, vol. 13, no. 14, pp. 2960–2970, 2020.
- [56] H. Heydari-doostabad and T. O'Donnell, "A Wide-Range High-Voltage-Gain Bidirectional DC-DC Converter for V2G and G2V Hybrid EV Charger," *IEEE Transactions on Industrial Electronics*, vol. 69, pp. 4718–4729, may 2022.
- [57] K. Shi, T. Q. Dinh, and J. Marco, "Dynamic Modelling of the Bidirectional Active Clamp Forward Converter with Peak Current Mode Control for Active Cell Balancing," in *2019 23rd International Conference on Mechatronics Technology (ICMT)*, pp. 1–7, IEEE, oct 2019.
- [58] F. J. Gomez Navarro, L. J. Yebra, F. J. Gomez Medina, and A. Gimenez-Fernandez, "DC-DC Linearized Converter Model for Faster Simulation of Lightweight Urban Electric Vehicles," *IEEE Access*, vol. 8, pp. 85380–85394, 2020.
- [59] F. Karakaya, Ö. Gülsuna, and O. Keysan, "Feasibility of Quasi-Square-Wave Zero-Voltage-Switching Bi-Directional DC/DC Converters with GaN HEMTs," *Energies*, vol. 14, p. 2867, may 2021.
- [60] F. Jin, A. Nabih, C. Chen, X. Chen, Q. Li, and F. C. Lee, "A High Efficiency High Density DC/DC Converter for Battery Charger Applications," in *2021 IEEE Applied Power Electronics Conference and Exposition (APEC)*, pp. 1767–1774, IEEE, jun 2021.
- [61] G. R. Chandra Mouli, J. Schijffelen, M. Van Den Heuvel, M. Kardolus, and P. Bauer, "A 10 kW Solar-Powered Bidirectional EV Charger

- Compatible with Chademo and COMBO," *IEEE Transactions on Power Electronics*, vol. 34, no. 2, pp. 1082–1098, 2019.
- [62] J. S. Artal-Sevil, V. Ballester-Bernad, J. Anzola, and J. A. Dominguez-Navarro, "High-Gain Non-isolated DC-DC Partial-Power Converter for Automotive Applications," in *2021 IEEE Vehicle Power and Propulsion Conference (VPPC)*, pp. 1–6, IEEE, oct 2021.
- [63] S. A. Assadi, H. Matsumoto, M. Moshirvaziri, M. Nasr, M. S. Zaman, and O. Trescases, "Active Saturation Mitigation in High-Density Dual-Active-Bridge DC-DC Converter for On-Board EV Charger Applications," *IEEE Transactions on Power Electronics*, vol. 35, pp. 4376–4387, apr 2020.
- [64] D. Zhang, M. Guacci, M. Haider, D. Bortis, J. W. Kolar, and J. Everts, "Three-Phase Bidirectional Buck-Boost Current DC-Link EV Battery Charger Featuring a Wide Output Voltage Range of 200 to 1000V," *ECCE 2020 - IEEE Energy Conversion Congress and Exposition*, pp. 4555–4562, 2020.
- [65] F. Caricchi, F. Crescimbin, F. Capponi, and L. Solero, "Study of bi-directional buck-boost converter topologies for application in electrical vehicle motor drives," in *APEC '98 Thirteenth Annual Applied Power Electronics Conference and Exposition*, vol. 1, pp. 287–293, IEEE, 1998.
- [66] M. A. Khan, A. Ahmed, I. Husain, Y. Sozer, and M. Badawy, "Performance Analysis of Bidirectional DC-DC Converters for Electric Vehicles," *IEEE Transactions on Industry Applications*, vol. 51, no. 4, pp. 3442–3452, 2015.
- [67] S. Chakraborty, M. Mazuela, D. D. Tran, J. A. Corea-Araujo, Y. Lan, A. A. Loiti, P. Garmier, I. Aizpuru, and O. Hegazy, "Scalable Modeling Approach and Robust Hardware-in-the-Loop Testing of an Optimized Interleaved Bidirectional HV DC/DC Converter for Electric Vehicle Drivetrains," *IEEE Access*, vol. 8, pp. 115515–115536, 2020.
- [68] S. Chakraborty, M. M. Hasan, D. Duong Tran, S. Jaman, P. Van Den Bossche, M. El Baghdadi, and O. Hegazy, "Reliability Assessment of a WBG-based Interleaved Bidirectional HV DC/DC Converter for Electric Vehicle Drivetrains," *2020 15th International Conference on Ecological Vehicles and Renewable Energies, EVER 2020*, 2020.
- [69] "High-power high-voltage 200kW 10V to 1200V 250A bi-directional DC/DC."
- [70] "Fraunhofer Institute for Integrated Systems and Device Technology IISB."
- [71] "Bidirectional dc power supply Jinan ACME Power Supply Co.,Ltd."
- [72] B. Choi, *Pulsedwidth Modulated DC-to-DC Power Conversion*. Hoboken, NJ, USA: John Wiley & Sons, Inc., jul 2013.
- [73] L. Wang, S. Chai, D. Yoo, L. Gan, and K. Ng, *PID and Predictive Control of Electrical Drives and Power Converters Using MATLAB®/SIMULINK®*. Singapore: John Wiley & Sons Singapore Pte. Ltd., 2015.
- [74] F. B. Lynser, M. Sun, M. Sungoh, N. Taggu, and P. Konwar, "Comparative Analysis of Different Control Schemes for DC-DC Converter: A Review," *ADBU Journal of Electrical and Electronics Engineering (AJEEE)*, vol. 2, no. 1, pp. 8–13, 2018.
- [75] M. Lešo, J. Žilková, M. Biroš, and P. Talian, "Survey of Control Methods for DC-DC Converters," *Acta Electrotechnica et Informatica*, vol. 18, pp. 41–46, sep 2018.
- [76] Q. Qi, D. Ghaderi, and J. M. Guerrero, "Sliding mode controller-based switched-capacitor-based high DC gain and low voltage stress DC-DC boost converter for photovoltaic applications," *International Journal of Electrical Power and Energy Systems*, vol. 125, no. September 2020, p. 106496, 2021.
- [77] V. Utkin, A. Poznyak, Y. Orlov, and A. Polyakov, "Conventional and high order sliding mode control," *Journal of the Franklin Institute*, vol. 357, no. 15, pp. 10244–10261, 2020.
- [78] K. Shi, T. Bui, and J. Marco, "Optimal control of bidirectional active clamp forward converter with synchronous rectifier based cell-to-external-storage active balancing system," *Journal of Energy Storage*, vol. 41, p. 102851, sep 2021.
- [79] J. Chen, Y. Chen, L. Tong, L. Peng, and Y. Kang, "A Backpropagation Neural Network-Based Explicit Model Predictive Control for DC-DC Converters with High Switching Frequency," *IEEE Journal of Emerging and Selected Topics in Power Electronics*, vol. 8, no. 3, pp. 2124–2142, 2020.
- [80] B. Chelladurai, C. K. Sundarabalan, S. N. Santhanam, and J. M. Guerrero, "Interval Type-2 Fuzzy Logic Controlled Shunt Converter Coupled Novel High-Quality Charging Scheme for Electric Vehicles," *IEEE Transactions on Industrial Informatics*, vol. 17, no. 9, pp. 6084–6093, 2021.
- [81] M. Fu, C. Fei, Y. Yang, Q. Li, and F. C. Lee, "A GaN-Based DC-DC Module for Railway Applications: Design Consideration and High-Frequency Digital Control," *IEEE Transactions on Industrial Electronics*, vol. 67, no. 2, pp. 1638–1647, 2020.
- [82] S. M. Miraftebadeh, F. Foaidelli, M. Longo, and M. Pasetti, "A Survey of Machine Learning Applications for Power System Analytics," *Proceedings - 2019 IEEE International Conference on Environment and Electrical Engineering and 2019 IEEE Industrial and Commercial Power Systems Europe, IEEEIC/ and CPS Europe 2019*, 2019.
- [83] A. Kumbhar, P. G. Dhawale, S. Kumbhar, U. Patil, and P. Magdum, "A comprehensive review: Machine learning and its application in integrated power system," *Energy Reports*, vol. 7, pp. 5467–5474, 2021.
- [84] M. Farhoumandi, Q. Zhou, and M. Shahidehpour, "A review of machine learning applications in IoT-integrated modern power systems," *Electricity Journal*, vol. 34, no. 1, p. 106879, 2021.
- [85] Y.-X. Wang, F.-F. Qin, and Y.-B. Kim, "Bidirectional DC-DC converter design and implementation for lithium-ion battery application," in *2014 IEEE PES Asia-Pacific Power and Energy Engineering Conference (APPEEC)*, vol. 2015-March, pp. 1–5, IEEE, dec 2014.
- [86] S. Talbi, A. M. Mabwe, and A. E. Hajjaji, "Control of a bidirectional dual active bridge converter for charge and discharge of a Li-Ion Battery," *IECON 2015 - 41st Annual Conference of the IEEE Industrial Electronics Society*, pp. 849–856, 2015.
- [87] G. Gurjar, D. K. Yadav, and S. Agrawal, "Illustration and Control of Non-Isolated Multi-Input DC - DC Bidirectional Converter for Electric Vehicles Using Fuzzy Logic controller," *2020 IEEE International Conference for Innovation in Technology, INOCON 2020*, pp. 2–6, 2020.
- [88] V. Michal, "Optimal Load Transient Response of the Boost DC-DC Converter Based on Stochastic Duty-cycle Sequence Generator," *2021 31st International Conference Radioelektronika, RADIOELEKTRONIKA 2021*, 2021.
- [89] F. Kurokawa, H. Maruta, T. Mizoguchi, A. Nakamura, and H. Osuga, "A New Digital Control DC-DC Converter with Multi-layer Neural Network Predictor," in *2009 International Conference on Machine Learning and Applications*, pp. 638–643, IEEE, dec 2009.
- [90] J. Ramirez-Hernandez, O. U. Juarez-Sandoval, L. Hernandez-Gonzalez, A. Hernandez-Ramirez, and R. S. Olivares-Dominguez, "Voltage Control Based on a Back-Propagation Artificial Neural Network Algorithm," *2020 IEEE International Autumn Meeting on Power, Electronics and Computing, ROPEC 2020*, no. ROPEC, 2020.
- [91] S. Saadatmand, M. Kavousi, and S. Azizi, "The Voltage Regulation of Boost Converters Using Dual Heuristic Programming," in *2020 10th Annual Computing and Communication Workshop and Conference (CCWC)*, pp. 0531–0536, IEEE, jan 2020.
- [92] J. Chen, Y. Chen, and Y. Kang, "A Real-Time Self-Learning Control for Megahertz GaN-based DC-DC Converter," *IEEE Workshop on Wide Bandgap Power Devices and Applications in Asia, WIPDA Asia 2021*, pp. 157–161, 2021.
- [93] "Nissan March 2023 | Nissan México."
- [94] "Auto Sedán Aveo | Motor 1.5L con 107 HP | Chevrolet Mex."
- [95] "Autos eléctricos nuevos y usados | Tesla México."
- [96] "LEAF® | Nissan México."
- [97] "Silicon Carbide Power & GaN RF Solutions | Wolfspeed."
- [98] "Where to buy | GaN Systems."
- [99] "ROHM Semiconductor - ROHM Co., Ltd."
- [100] "Findchips: Electronic Part Search."
- [101] "Electronic Components Distributor - Mouser Electronics."
- [102] "Electronic Components Online | Find Electronic Parts | Arrow.com."
- [103] "Search for Electronic Component's Price & Stock | DigiPart."
- [104] "Semiconductor & System Solutions - Infineon Technologies."



Erik Martinez-Vera received his BSc. degree in Electronics Engineering from Universidad de las Américas-Puebla, México, in 2003. He was an Associate Technical Professional with major Energy Companies from 2004 to 2015. Results of his work were published in major International Technical Conferences. Looking forward to contribute to a sustainable development, in 2017 he received his MSc. degree in Sustainable Automotive Engineering from Warwick University, UK. Currently, he is a PhD visiting student at the Universitat de València, Spain and a Ph.D. candidate in the Intelligent Systems program in Universidad de las Américas-Puebla, México. His research interest include Power Electronics, Electric Vehicles, Systems Control and Intelligent Systems.



Dr. Pedro Bañuelos-Sánchez received the Ph.D. degree in electrical engineering from the Ecole Supérieure d'Electricité, Paris, France, in 2001. He is currently a Professor with the Department of Computation, Electronics and Mechatronics, Universidad de las Américas Puebla, San Andrés Cholula, México. He was an Associate Researcher, Visiting Researcher, and Visiting Professor with different universities. His research interests include high-frequency power conversion, power factor correction techniques, high-frequency magnetics, power converters applied to photovoltaic and wind energy, and modeling and control of converters.